Supplementary information

Radio frequency plasma characterization

To characterize the plasma created inside the plasma cleaner, a Langmuir probe with a planar, circular surface was built, which could be inserted electrically isolated from the plasma cleaner. A photograph of the probe is shown in Figure S1, we point out that it was designed in such a way, that the probe is in the same position as a sample in the TEM holder when inserted. Using a KEITHLEY 2450 SourceMeter a voltage sweep from -200 to +200 V was applied, while measuring the current. A characteristic I-U curve is shown in Figure S2. The floating point potential V_f is reached when electron and ion flow to the probe is equal and thus no net current to the probe exists. It can be determined at the intersection of the graph and the x-axis, as shown in Figure S2. At voltages below V_f the ion saturation current can be found. The electron saturation region lies at voltages higher than the plasma potential V_s . To determine V_s , the logarithm from the I-U curve is taken and two linear regressions fitted to the electron saturation region and the exponential growth of the electron current. The intersection of the two lines denotes V_s , as shown in Figure S2. From the region between V_f and V_s the electron temperature T_e can be extracted by fitting the exponential current rise [1,2]:

$$\ln(I) = \frac{V_e}{k_B T_e} + \text{constants} \tag{1}$$

where I is the measured current, V the applied voltage, e the elementary charge and k_B the Boltzmann constant. The plasma density n_0 can be determined from

$$I = A\left(\frac{en_0v_e}{4}\right) \quad \text{with} \quad v_e = \left(\frac{8k_BT_e}{\pi m_e}\right) \tag{2}$$

with the probe surface A, the electron speed v_e and electron mass m_e . The plasma density usually refers to the electron density n_e , but because of the quasineutrality $n_e = n_0 = n_I$ applies and allows us to extract the ion density n_I . Table S1 shows the determined values T_e and n_I from different plasma settings used to dope the samples in this work.

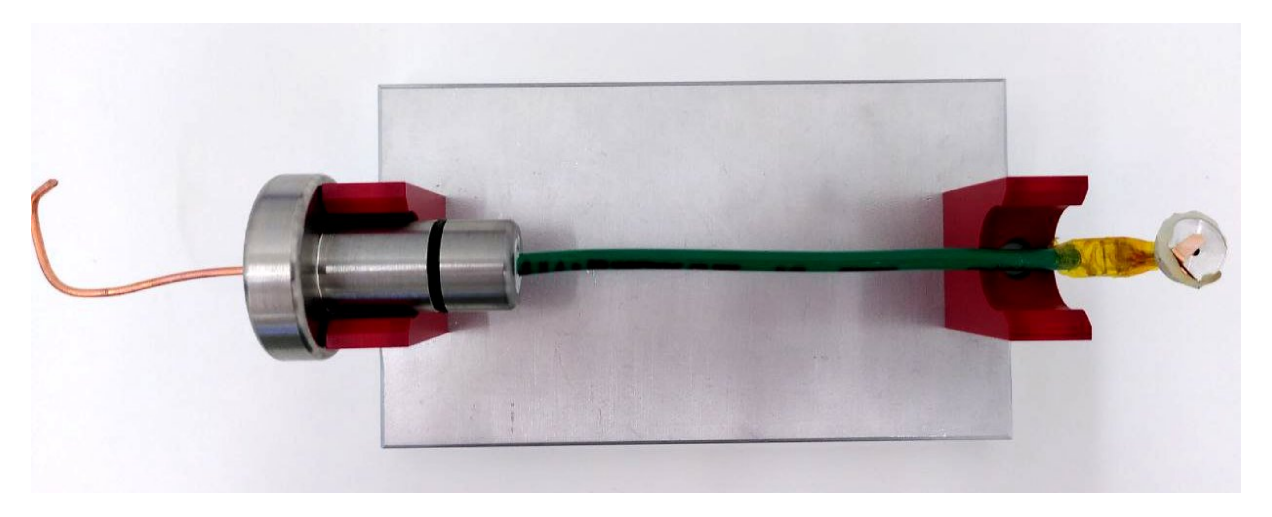
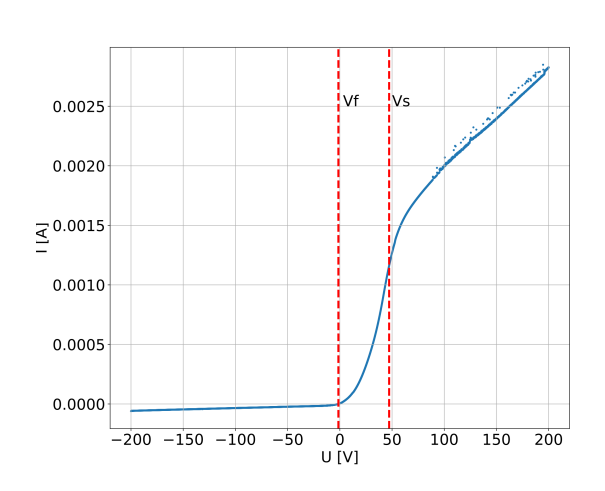


Figure S1: Langmuir probe used for characterization of plasma. It even allows to attach samples to it if needed.

Table S1: Calculated electron temperatures T_e and ion density n_I for different RF plasma settings.

Parameters	T_e [eV]	$n_I \left[\frac{1}{\mathrm{cm}} \right]$
1 W/1 sccm	13.54	$1.50\cdot 10^8$
1 W/25 sccm	10.65	$5.67 \cdot 10^{7}$
1 W/ 50 sccm	8.15	$4.97\cdot 10^7$



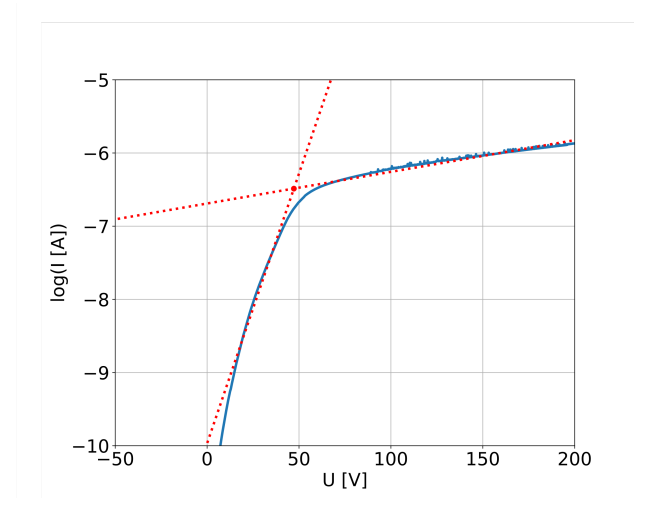


Figure S2: Left: I-U curve for RF plasma with 1 W power and 1 sccm gas flow. Floating potential V_f and plasma potential V_s are marked. Right: Logarithm of I-U curve with two linear fits to determine V_s .

Direct current gas discharge plasma characterization

To better handle the DC plasma inside the self built chamber, some tests were done. Figure S3 shows discharges at three different pressures. 0.3 mbar was the lowest pressure were ignition was possible. During experimentation it was found that short plasma pulses give the most reliable results. To measure the time of one pulse, a video was recorded, Figure S4 shows selected frames from this recording. Paschen curves were recorded for two different electrode distances, as well as the voltage that stabilizes after breakdown (plasma voltage). The breakdown voltage is the voltage that needs to be applied to ignite a discharge and is important to properly use the setup [3,4]. Results are shown in Figure S5.



Figure S3: Light phenomena observed under DC gas discharge with N_2 gas at different pressures.

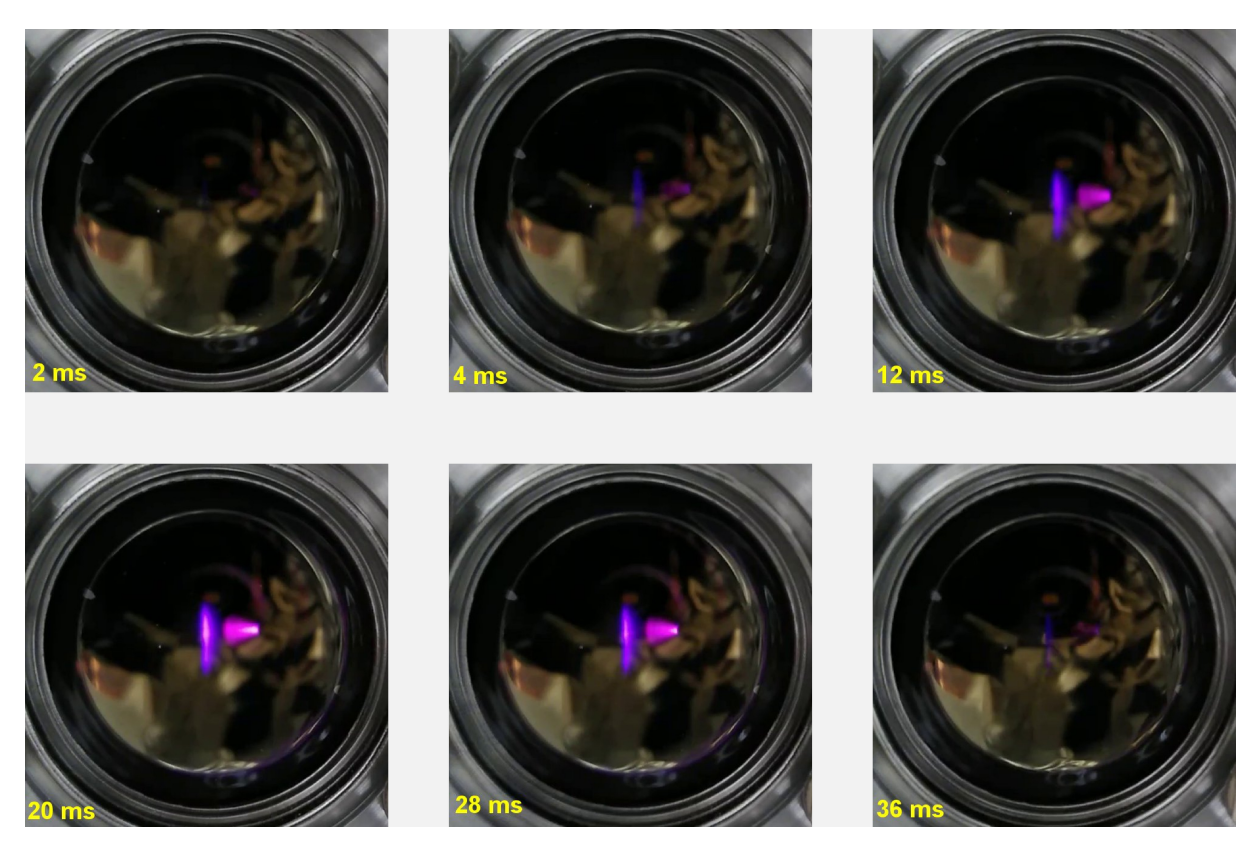


Figure S4: Sequence of images taken from a video of a plasma pulse at 6.5 mbar pressure. Time stamps are shown in lower left corner.

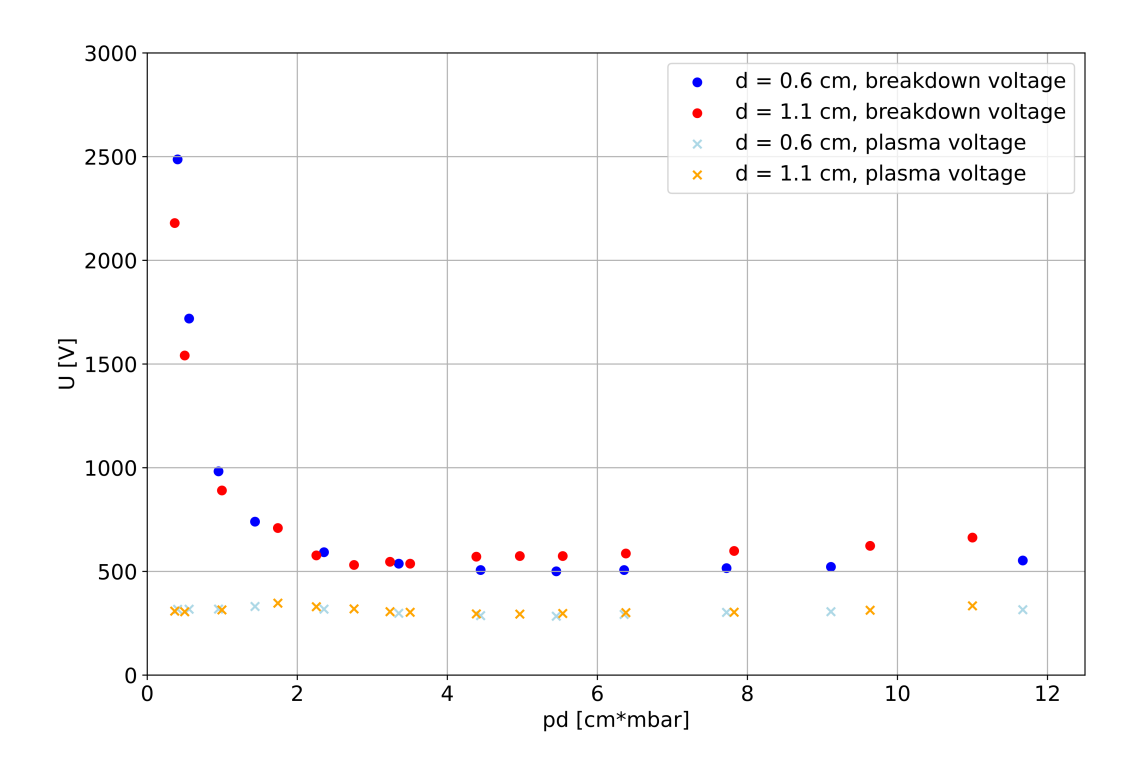


Figure S5: Paschen curves and plasma voltages for two different electrode distances.

Detecting graphitic nitrogen

Nitrogen substitutions in graphene exhibit a very weak contrast in comparison to carbon. In order to reach a sufficient signal to noise ratio, about 30 HRTEM images are summed. This is the starting image in Figure S6. To make them visible to the eye, the graphene lattice is removed by a Fourier filter, and the contrast of the image is increased. This also leads to small variations in the background intensity being amplified, and the contrast at and around contamination reaches the limits of the greyscale.

To confirm that the found defect is indeed graphitic nitrogen, the contrast change due to the defect is compared to HRTEM image simulations. Here, it is important that the simulations are based on accurate potentials that take into account the charge redistribution in the C-N bonds, as demonstrated in earlier work [5]. In this case, the experimental Figure S7) and simulated (Figure S8) intensity profiles are in excellent agreement.

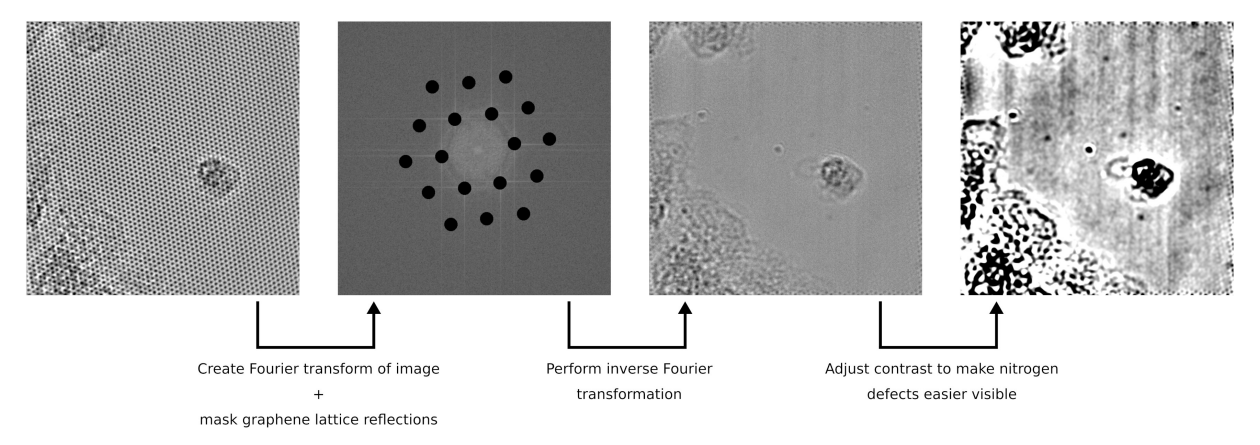
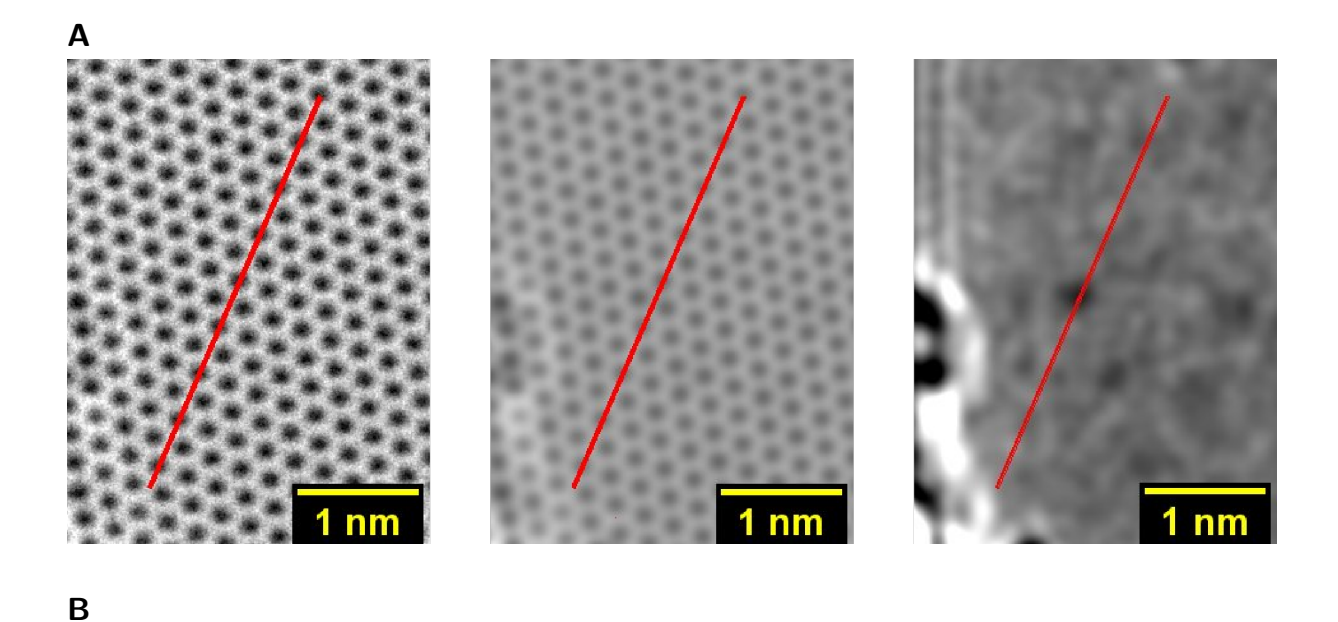


Figure S6: Procedure for removing the graphene lattice from the image, making graphitic nitrogen and other defects easier to detect by eye.



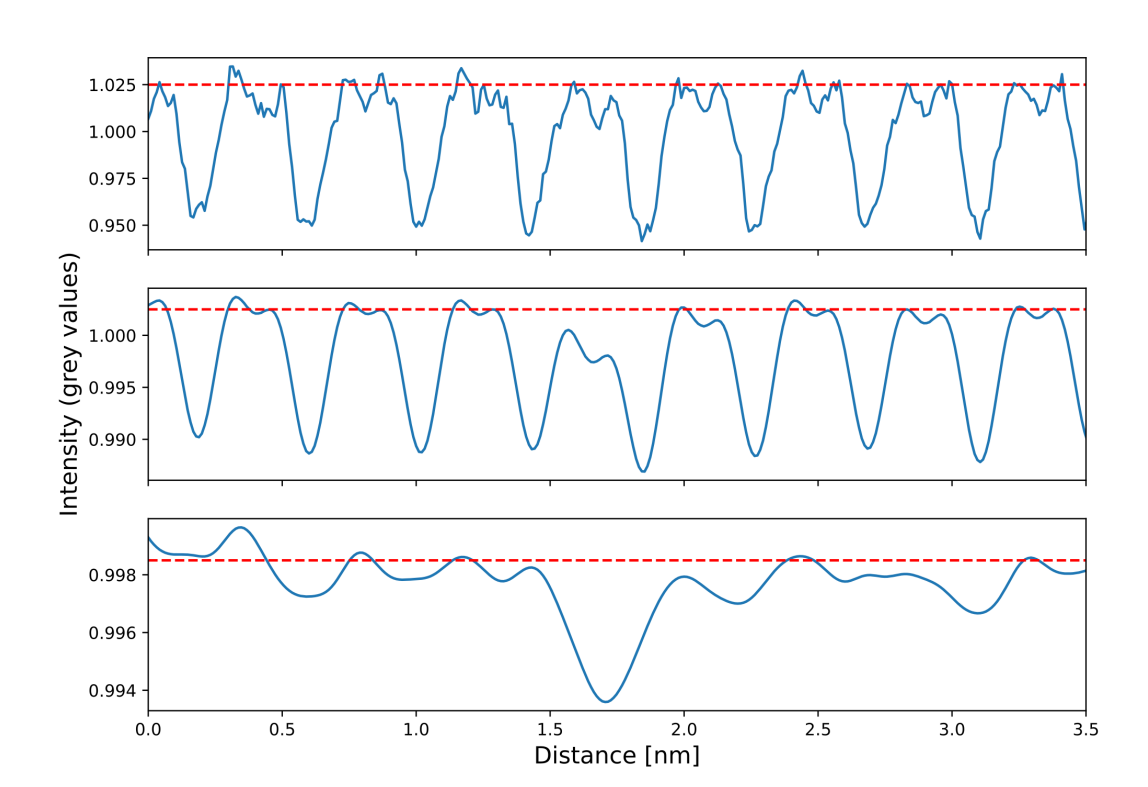
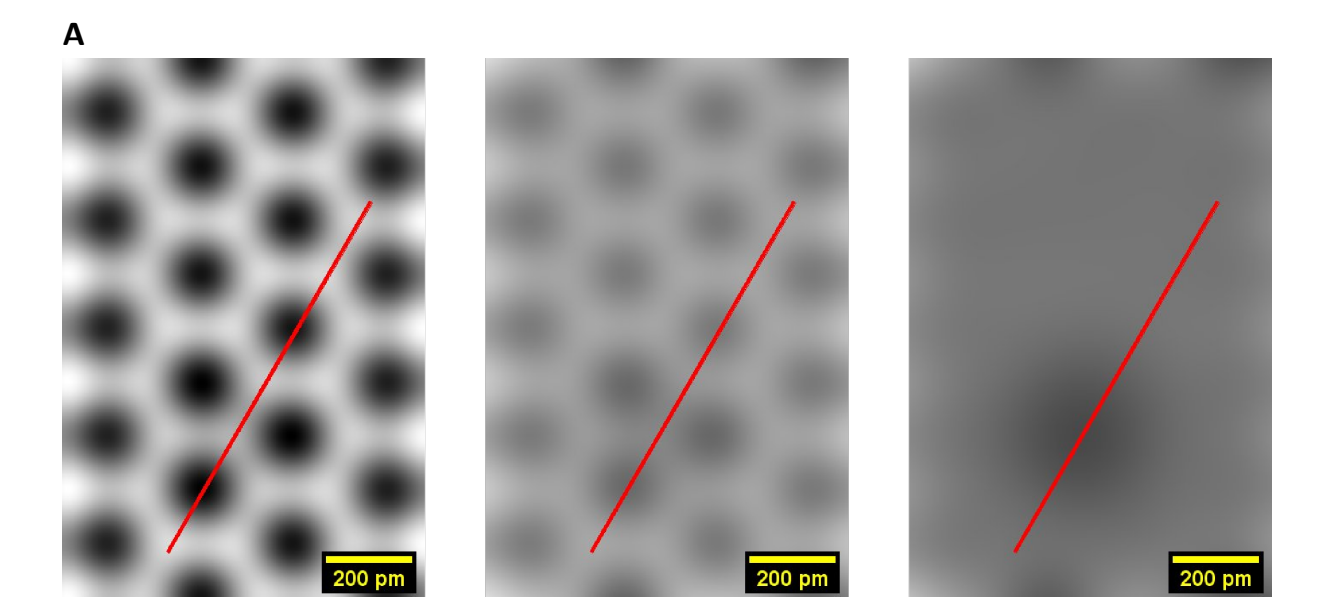


Figure S7: (A) Example of a line profile taken from a HRTEM image showing graphitic nitrogen (red line). The first image shows unfiltered data. To the second image, a Gauss blur was applied with the width chosen so that it reduces the contrast of the carbon lattice without removing it completely, making the contrast change due to the nitrogen more clear. In the third image the graphene lattice was filtered out, followed by a slight Gauss blur to remove pixel to pixel variations (left to right). (B) Corresponding line profiles from A, top one taken from left image and bottom one from right image.



В

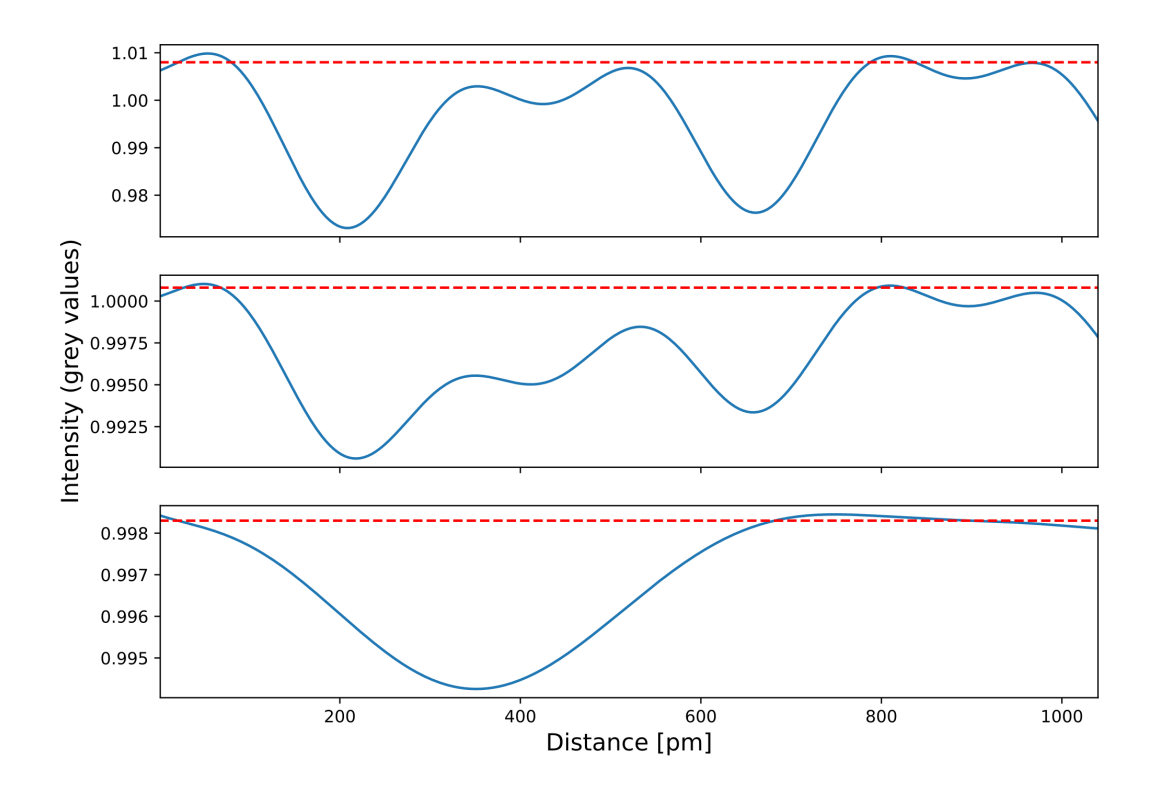
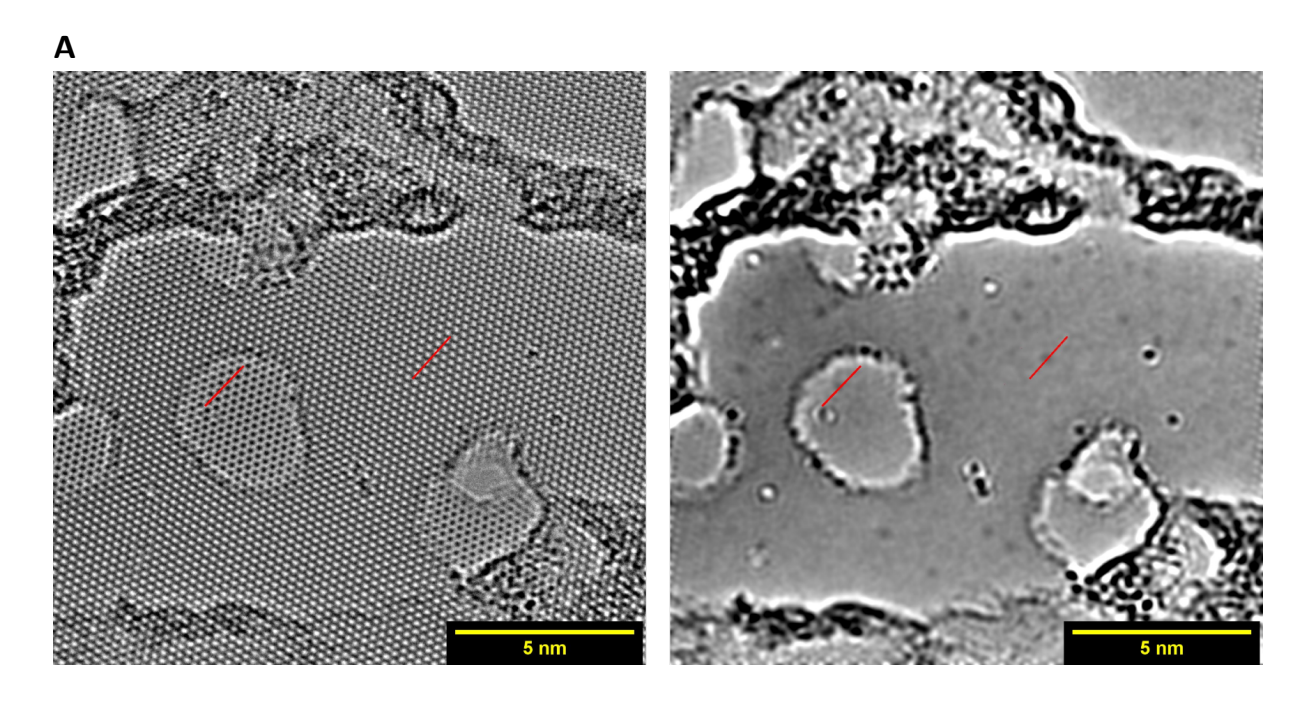


Figure S8: (A) Example of a line profile taken from simulation of a HRTEM image showing graphitic nitrogen (red line). The first image is unfiltered, in the second image a Gauss blur was applied and in the third image the graphene lattice was filtered out, followed by a slight Gauss blur (left to right). (B) Corresponding line profiles from A, top one taken from left image and bottom one from right image.

Bilayer graphene

To confirm the same behavior in in contrast change for graphitic nitrogen defects found in mono- and bilayer graphene, line profiles from nitrogen defects on both area were taken. The results are shown in Figure S9 and from the line profiles it can be confirmed, that in both regions the same contrast change occurs.



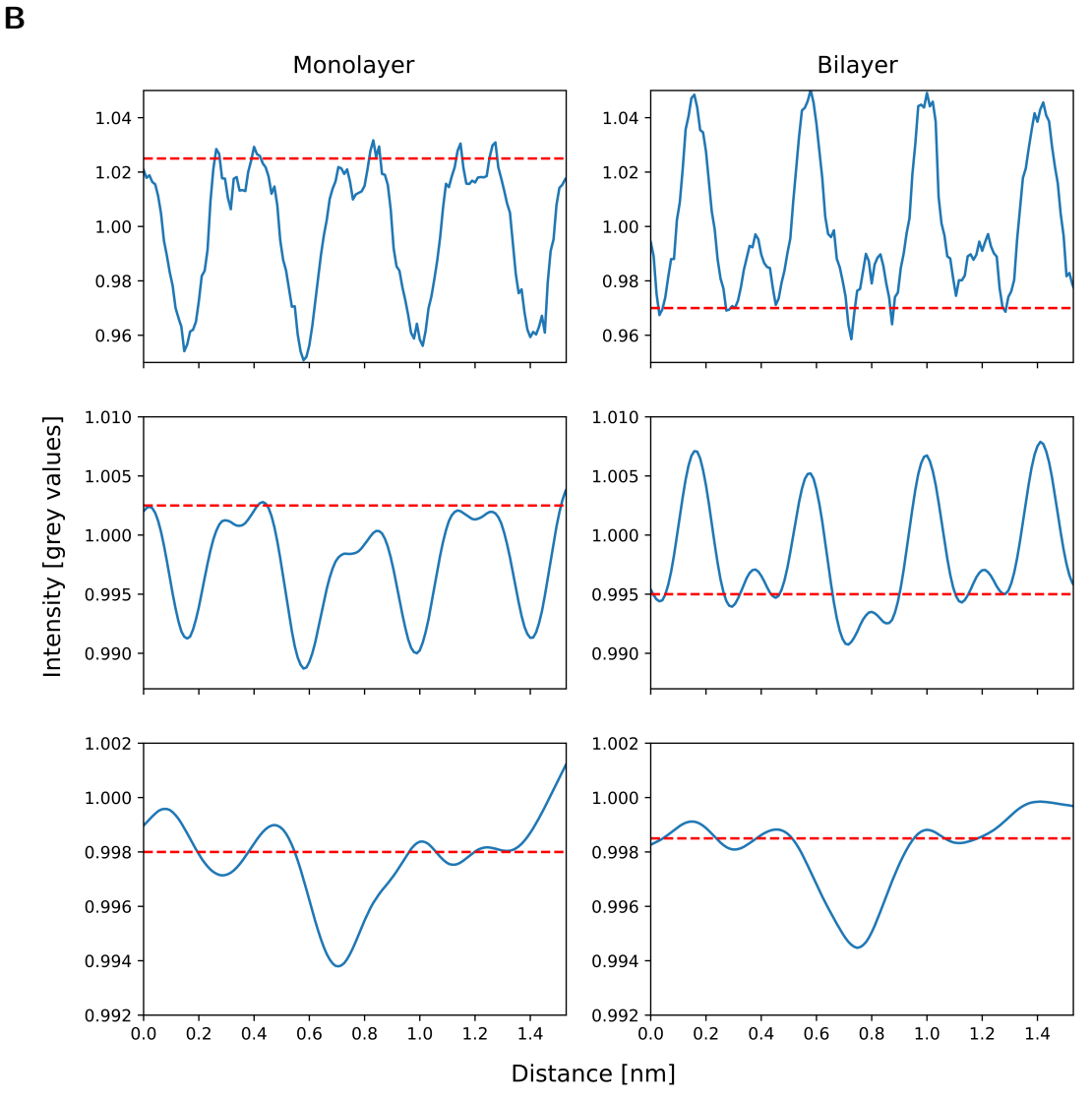


Figure S9: (A) HRTEM images taken from region with bilayer graphene doped with 2 pulses at 5 mbar. From nitrogen defects on monolayer (white atoms) and bilayer (dark atoms) region line profiles were taken (red line). (B) Line profiles taken from A. First row shows unfiltered data, for the second row a Gauss blur was applied to the image and for the third row the graphene lattice was filtered out followed by a slight Gauss blur.

Supplementary references

- [1] F. F. Chen, "Langmuir Probe Diagnostics," vol. 2, (Jeju, Korea), pp. 20–111, 2003.
- [2] P. Gibbon, "Introduction to Plasma Physics," CERN Yellow Reports, vol. 1, pp. 51–51, Feb. 2016.
- [3] K. T. a. L. Burm, "Calculation of the Townsend Discharge Coefficients and the Paschen Curve Coefficients," *Contributions to Plasma Physics*, vol. 47, no. 3, pp. 177–182, 2007.
- [4] B. M. Smirnov, *Theory of Gas Discharge Plasma*, vol. 84. Cham: Springer International Publishing, Jan. 2015.
- [5] J. C. Meyer, S. Kurasch, H. J. Park, V. Skakalova, D. Künzel, A. Groß, A. Chuvilin, G. Algara-Siller, S. Roth, T. Iwasaki, U. Starke, J. H. Smet, and U. Kaiser, "Experimental analysis of charge redistribution due to chemical bonding by high-resolution transmission electron microscopy," *Nature Materials*, vol. 10, pp. 209–215, Mar. 2011.